Thermal-Fluid Model of Meniscus Behavior during Mold Oscillation in Steel Continuous Casting

Xiaolu Yan, ASM Jonayat and Brian G. Thomas

Department of Mechanical Science and Engineering,
University of Illinois at Urbana-Champaign,
1206 West Green Street, IL, 61801
Phone: (217) 333-6919
Fax: (217) 244-6534
Email: bgthomas@illinois.edu

ABSTRACT

The surface quality of steel depends on initial solidification at the meniscus during continuous casting. A computational thermal-fluid model has been developed to simulate the complex transient behavior of the slag layer between the oscillating mold wall, the slag rim, the slag/liquid steel interface, and the solidifying steel shell. It includes transient heat transfer, multi-phase fluid flow, solidification of the slag and steel, and movement of the mold during an oscillation cycle. The model is validated with transient temperature measurements from a "mold simulator" lab experiment and with plant measurements of slag consumption. During an oscillation cycle, thermocouple variations depend on their location relative to the meniscus and the rate of heat flow increases greatly when steel overflows the meniscus. The model reveals new insights into the phenomena which govern initial solidification, oscillation mark formation, and surface defects in this process.

A. Background

Initial solidification in casting processes is critical to product quality and involves many complex, coupled phenomena, including multiphase, 3-D fluid flow, heat transfer, solidification, thermal-stress, microstructure and defect formation. Michel Rappaz and coworkers have contributed greatly to this field, especially in the modeling of microstructure [1] grain structure [2] segregation [3], and hot tearing [4]. In the present work, a computational model of fluid flow, heat transfer and solidification is applied to the meniscus region of the steel continuous-casting process to simulate oscillation mark formation and related phenomena.

B. Domain and Governing Equations

A two-dimensional two-phase (slag and steel) thermal-fluid model has been developed to predict transient incompressible fluid-flow and temperature in the region near the mold face and meniscus of a continuous slab caster, including the oscillating solid mold. Figure 1 shows the two domains of this model, which are coupled by the heat transfer across the vertically-moving interface between them. The mold domain is solid and contains the top of the copper mold adjacent to the fluid domain with a width of 20mm. Only the energy equation is solved in this domain for the 2D temperature field.

The fluid domain contains powder, molten slag, steel shell and molten steel in the meniscus region extending 100mm (width) from the mold wall and a length from 100mm below to 50mm above the tip of the solidifying steel shell (length). In this domain, a single set of momentum, continuity, and energy equations are solved on a fixed grid with temperature- and phase-dependent material properties using the k-ω SST model [5,6] for turbulence, and the Volume-Of-Fluid (VOF) method to find the phase fractions, by conserving and advecting the steel volume fraction, α_{Fe}, and finding the slag volume fraction from total mass conservation:

$$\frac{\partial \alpha_{Fe}}{\partial t} + \boldsymbol{v} \cdot \nabla \alpha_{Fe} = 0; \;\; \alpha_{Fe} + \alpha_{sl} = 1$$

Solidification is achieved by extraction of latent heat linearly over the solidification range.

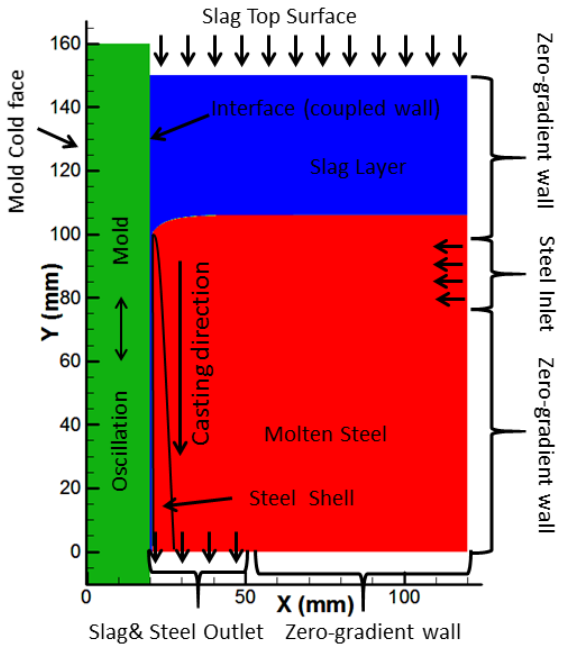

Fig. 1--Schematic of model domain and boundaries

The entire solid (mold) domain is prescribed a velocity according to the mold oscillation:

$$v_x = 0; \;\; v_y = v_m = \pi s f \sin\{2\pi f(t - t_0)\}$$

where s=stroke, f=frequency, t=time and t_0 is the time when the mold is just about to gain positive y velocity. Heat is extracted by convection from the mold cold face to the cooling water. The equations are solved using ANSYS Fluent, [7] as described elsewhere [11].

E. Material Properties

Slag enters the fluid domain as powder at the top surface (where pressure is fixed at 1atm and ambient temperature is 573K (300℃). During its travel downward, its temperature increases, so its viscosity increases as it sinters and melts, and then decreases. Some slag re-solidifies against the mold wall. The temperature-dependent slag properties shown in Fig. 2 depend on whether it is in the melting region (most of the domain), or re-solidifying region, found near the mold wall, $x \leq 23mm$. Slag density is fixed at 2500kg/m^3 [8].

The solid steel near its solidus temperature acts as a viscoplastic material, as its stress depends more on strain rate than strain. Thus, it is reasonable to model this steel with a power law fluid [9] with viscosity ~ $10^7\ Pa \cdot s$. However, to avoid convergence problems, the current model uses viscosity up to only $10^3\ Pa \cdot s$, (see Fig. 2), so rigidity of the steel after solidification is achieved by imposing a fixed-velocity boundary condition on the steel when its temperature $T \leq T_{solidus}$, and the steel volume fraction $\alpha_{Fe} \geq 0.8$.. Other properties are given in Table I.

Table I Properties of Steel and Cu (Mold)

Property/Material	*Steel*	*Cu (Mold)*	*Unit*
Density	*7000*	*8900*	kg/m^3
Specific heat	*700*	*385*	$J/kg\ K$
Thermal Conductivity	*30*	*350*	$W/m\ K$

Latent heat	2.72×10^5	—	J/kg
Solidus temp. $T_{solidus}$	*1802*	—	*K*
Liquidus temp. $T_{liquidus}$	*1803*	—	*K*

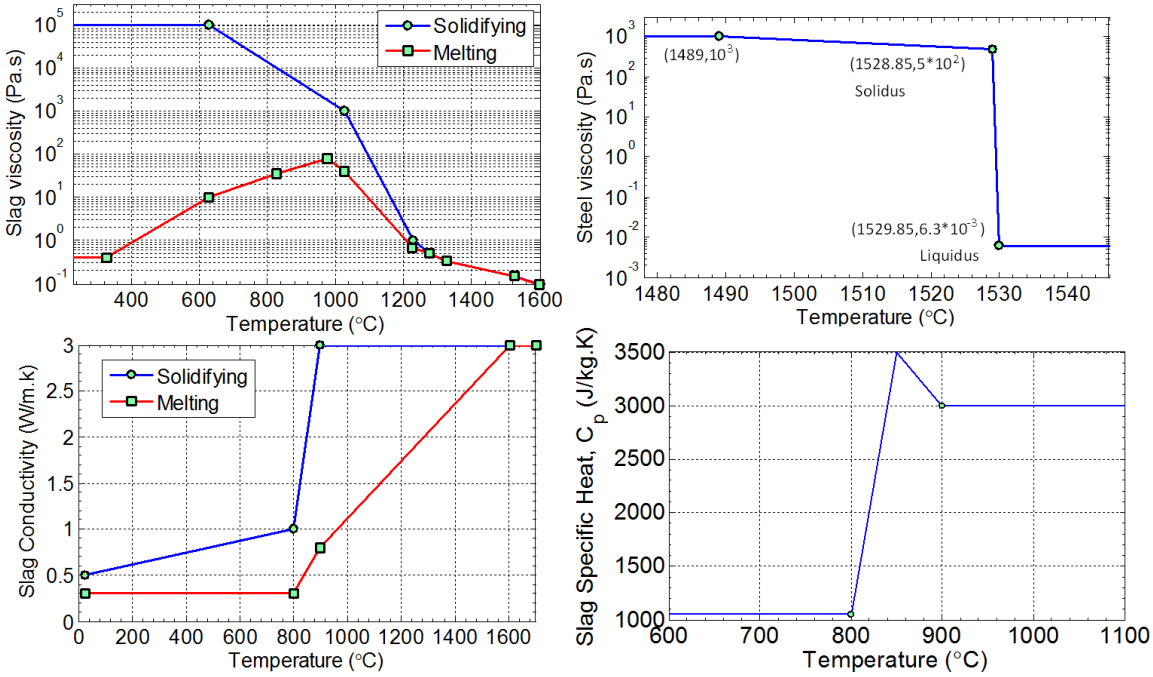

Fig. 2: Temperature dependent properties of slag and steel

G. Results

Results were obtained and presented below for typical continuous casting conditions of 1.39m/min casting speed, with an oscillation stroke of 5.89mm and frequency of 2.9Hz. The velocity of the"mass-flow rate" boundary [7] at the steel inlet in Fig. 1 was set to match the flow rate at the steel outlet (from x=20-45mm) in order to maintain constant liquid level at the far-field meniscus. The inlet temperature was 1806.5K, which corresponds to a superheat of 3.5K, which is low, as expected in the local meniscus region. Outlet pressure was 8358Pa higher than ambient, according to the ferrostatic pressure.

1. Flow field results

The velocity and temperature field variations for one oscillation cycle are shown in Fig. 3 (a) - (h), starting from (a) with zero displacement and the mold moving downward at maximum velocity. The downward moving slag rim squeezes slag into the gap and pushes the interfacial meniscus downward as shown in Fig. 3(b). The mold reaches its lowest position with zero velocity in Fig. 3 (c). The slag rim is pushed closest to the meniscus, causing a low steel level in meniscus region so steel far away from the meniscus starts to fill in. The mold moves upward in Figs. 3 (d) - (f), with maximum upward velocity at 8.32 sec. During this time, the slag rim pulls on the meniscus, causing molten steel to overflow the existing partly-solidified shell tip, and solidifies against the mold to form the new shell. A depression forms at the location of overflow, which corresponds to an oscillation mark that is carried down with the moving shell (strand) at the casting speed. This sequence of flow variation is repeated for every oscillation cycle, producing periodic oscillation marks. This "overflow" mechanism for oscillation mark formation is consistent with that proposed in previous work [10].

A close-up snapshot of the shape of the solidifying steel is shown in Fig. 4 by plotting the phase fractions colored according to region from the left (dark blue = solid copper mold; red = slag in the interfacial gap; dark blue = solid steel; red with arrows = liquid steel). The liquid steel has just overflowed the partly-solidified meniscus, which later is manifested as a

microstructural feature called a “hook” [10]. The bottom of the overflowed region forms the top of the oscillation mark.

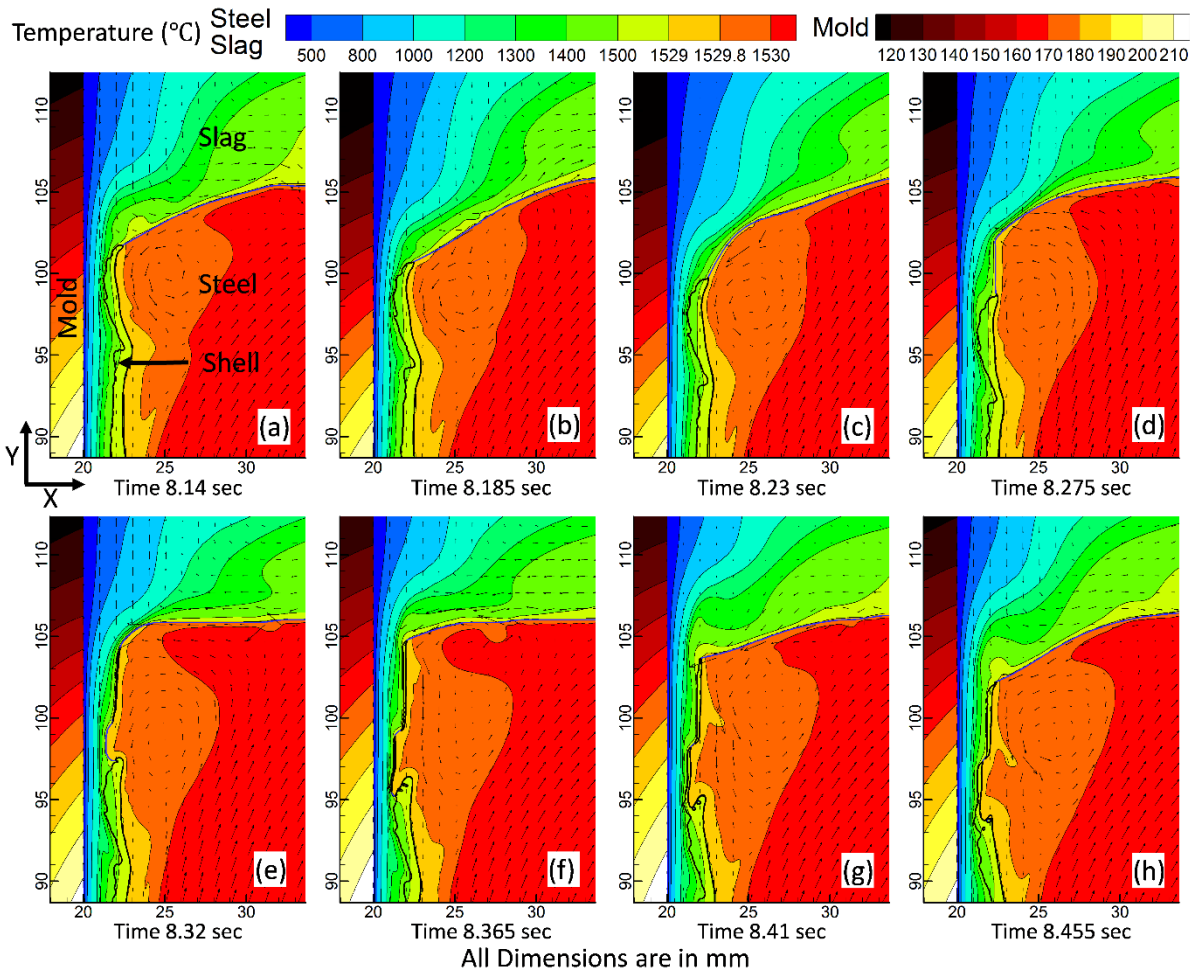

Fig. 3: Meniscus region events over one oscillation cycle

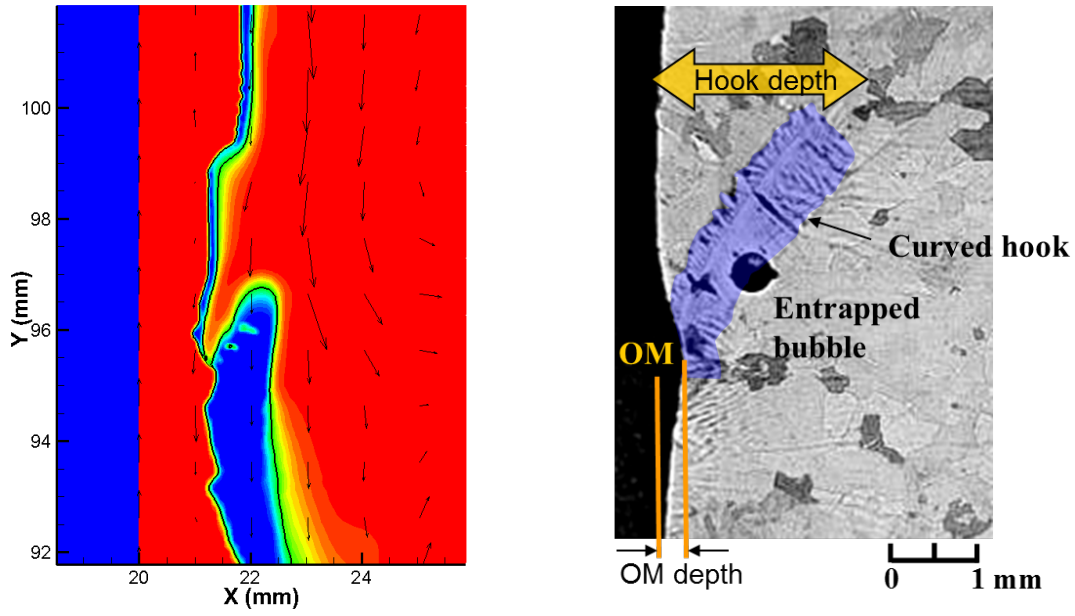

Fig. 4: Closeup of calculated oscillation mark and shell near meniscus showing subsurface hook created by overflow, compared with photograph of as-cast microstructure [10]

2. Shell strand surface profile

Figure 5 compares the strand surface profile at 3 different times, showing the depth and shape of the oscillation marks. The three profiles are plotted in the strand frame of reference, where $Y_s = 0$ is the location of the mean (far-field) surface level at 9.79s. The 3 profiles from the Eulerian model were translated according to the casting speed in order to have the same Y_s value at the same position along the shell surface at the 3 times. The three profiles compare reasonably well, which shows that oscillation mark shape does not evolve much after they form. Each peak on the profile represents the root of an oscillation mark. The pitch is calculated to be 7.82mm with a standard deviation of 0.94mm, while the theoretical pitch is 8.01mm. This variation is typical of measurements.

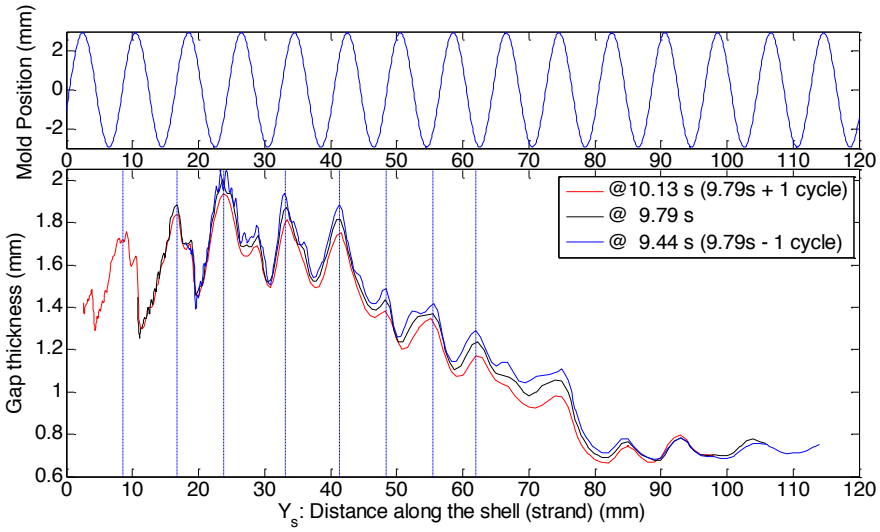

Fig. 5: Predicted strand surface profile at 3 different times, (translated according to the casting speed to compare the surface shape evolution)

3. Slag consumption

Figure 6 shows the variation in slag consumption over 7 oscillation cycles. Instantaneous

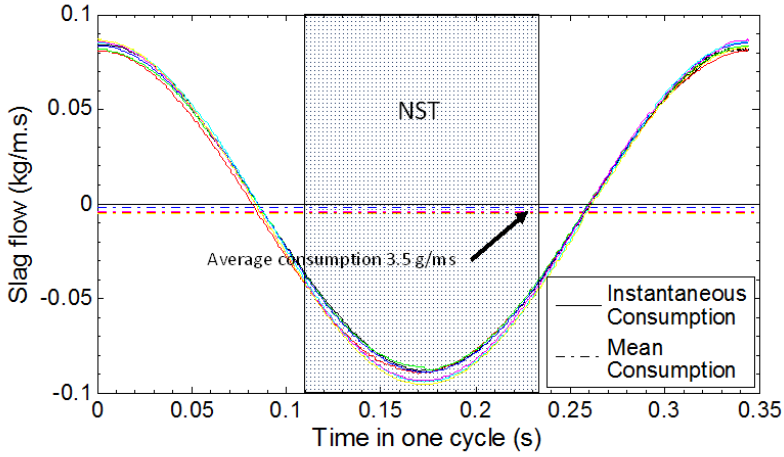

Cycle #	1	2	3	4	5	6	7	Average
Mean Consumption	2.3	4.6	2.2	2.3	3.8	3.8	5.3	3.5

Fig. 6: Predicted instantaneous and mean slag consumption

consumption various in a sinusoidal form, showing how slag consumption is mainly controlled by the oscillating slag rim. The rim pushes slag into the gap during the downstroke, but is drawn out during the upstroke. The net average consumption over 7 cycles is predicted to be 3.5g/ms, which is much smaller than the variations, but is typical of plant measurements [8].

4. Heat flux

Figure 7 shows the predicted transient heat flux profile over an oscillation cycle. Temperature rises steeply with distance below the far-field meniscus (x=0). The exact location of this steep region moves with the oscillating mold wall, so occurs further down below the meniscus, when the mold is lower (bottom of downstroke). Both the shape of the profile and the maximum of ~2.5-3.0 MW/m^2 are typical of that found in conventional steel slab casting [8,11].

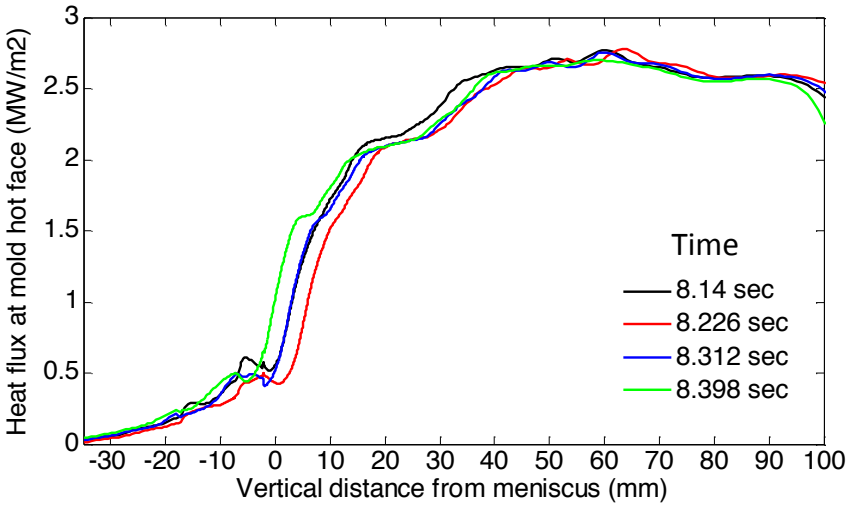

Fig. 7: Predicted transient heat flux profile over an oscillation cycle

References

1. Rappaz, M., Gandin, Ch.-A. Acta Metallurgica et Materialia, **41**(2), 1993, 345-360.
2. Gandin, Ch.-A., Desbiolles, J.-L., Rappaz, M., Thévoz, Ph., Metal. Mater. Trans. A, **30** (12), 1999, 3153-3165.
3. Kajitani, T., Drezet, J.-M., Rappaz, M. Metal. Mater. Trans. A, **32**(6), 2001, 1479-91.
4. Rappaz, M., J-M Drezet, M. Gremaud, Metal. Mater. Trans. A, **30**(2), 1999, 449-455.
5. F.R. Menter: AIAA J., **32**, 1994, 1598–1605.
6. F.R. Menter, M. Kuntz, R. Langtry: Turb. Heat Mass Transfer, **4,** 2003, 625–32.
7. ANSYS Fluent. 13.0, Canonsburg, PA, 2013.
8. H.-J. Shin, S.H. Kim, B.G. Thomas, G.G. Lee, J.M. Park, and J.Sengupta: ISIJ Int., **46**, 2006, 1635–44.
9. B.G. Thomas and J.T. Parkman: Thermec '97, TMS Conf. on Thermomechanical Processing of Steel and Other Materials, Wollongong, Australia, **2,** 1997, 2279-85.
10. Sengupta, J., H.-J. Shin, B.G. Thomas, S.-H. Kim, Acta Materialia, **54**(4), 2006, 1165-73.
11. ASM Jonayat, and B.G. Thomas, Metal. Mater. Trans. B, **45**(5), 2014, 1842-64.